

20 dB Net-Gain Polarization-Insensitive Fiber Optical Parametric Amplifier with >2 THz Bandwidth

M. F. C. STEPHENS,* V. GORDIENKO, AND N. J. DORAN

Aston Institute of Photonic Technologies, Aston University, Aston Triangle, Birmingham, U.K., B4 7ET
[*m.stephens@aston.ac.uk](mailto:m.stephens@aston.ac.uk)

Abstract: A black-box polarization insensitive fiber optical parametric amplifier (PI-FOPA) is characterized for the first time using a commercial 127 Gb/s polarization-division multiplexed PDM-QPSK transponder within a multiplex of twenty-two equivalent DWDM signals across a 2.3 THz bandwidth portion of the C-band. The PI-FOPA employs a recently demonstrated diversity loop arrangement comprising two lengths of highly nonlinear fiber (HNLF) with the parametric pump being removed after the first HNLF in both directions about the loop. This arrangement is named the Half-Pass Loop FOPA or HPL-FOPA. In total, a record equivalent 2.3 Tb/s of data is amplified within the HPL-FOPA for three different pump power regimes producing net-gains of 10 dB, 15 dB and 20 dB (averaged over all signals). For the latter two regimes, the gain bandwidth is observed to extend considerably beyond the C-band, illustrating the potential for this design to amplify signals over bandwidths commensurate with the EDFA and beyond. Under the 15 dB gain condition, the average OSNR penalty to achieve 10^{-3} bit error rate for all twenty three signals was found to be 0.5 ± 0.3 dB. Worst case penalty was 0.8 ± 0.3 dB, verifying the use of the architecture for polarization insensitive operation. The growth of four-wave mixing signal-signal crosstalk is additionally characterized and found to be gain independent for a fixed output power per signal. A simple effective length model is developed which predicts this behavior and suggests a new configuration for significantly reduced crosstalk.

© 2017 Optical Society of America

OCIS codes: Fiber optics amplifiers and oscillators; (060.2330) Fiber optics communications; 190.4410 Nonlinear optics, parametric processes.

References and links

1. V. Gordienko, M. F. C. Stephens, A. E. El-Taher, and N. J. Doran, "Ultra-flat wideband single-pump Raman-enhanced parametric amplification," *Opt. Express* **25**(5), 4810–4818 (2017).
2. R. Stolen, and J. Bjorkholm, "Parametric amplification and frequency conversion in optical fibers," *IEEE J. Quantum Electron.* **18**(7), 1062–1072 (1982).
3. M. E. Marhic, N. Kagi, T. K. Chiang, and L. G. Kazovsky, "Broadband fiber optical parametric amplifiers," *Opt. Lett.* **21**(8), 573–575 (1996).
4. T. Torounidis, and P. Andrekson, "Broadband single-pumped fiber-optic parametric amplifiers," *IEEE Photonics Technol. Lett.* **19**(9), 650–652 (2007).
5. K. K. Y. Wong, M. E. Marhic, K. Uesaka, and L. G. Kazovsky, "Polarisation-Independent Two-Pump Fibre-Optical Parametric Amplifier," *IEEE Photon. Technol. Lett.* **14**(7), 911–913 (2002).
6. J. M. C. Boggio, S. Moro, E. Myslivets, J. R. Windmiller, N. Alic, and S. Radic, "155-nm continuous-wave two-pump parametric amplification," *IEEE Photonics Technol. Lett.* **21**(10), 612–614 (2009).
7. H. Hu, R. M. Jopson, A. H. Gnauck, M. Dinu, S. Chandrasekhar, C. Xie, and S. Randel, "Parametric Amplification, Wavelength Conversion, and Phase Conjugation of a 2.048-Tbit/s WDM PDM 16-QAM Signal," *J. Lightw. Technol.* **33**(7), 1286–1291 (2014).
8. Q. Lin, and G. P. Agrawal, "Vector theory of four-wave mixing: polarization effects in fiber-optic parametric amplifiers," *J. Opt. Soc. Am. B* **21**(6), 1216–1224 (2004).
9. M. F. C. Stephens, M. Tan, I. D. Phillips, S. Sygletos, P. Harper, and N. J. Doran, "1.14 Tb/s DP-QPSK WDM polarization-diverse optical phase conjugation," *Opt. Express* **22**(10), 11840–11848 (2014).
10. I. Sackey, F. Da Ros, T. Richter, R. Elschner, M. Jazayerifar, C. Meuer, C. Peucheret, K. Petermann, and C. Schubert, "Design and performance evaluation of an OPC device using a dual-pump polarization-independent FOPA," in *European Conference on Optical Communication (ECOC 2014)*, paper Tu.1.4.4.

11. M. Jazayerifar, I. Sackey, R. Elschner, S. Warm, C. Meuer, C. Schubert, and K. Petermann, "Impact of SBS on Polarization-Insensitive Single-Pump Optical Parametric Amplifiers Based on a Diversity Loop Scheme," in *European Conference on Optical Communication (ECOC 2014)*, paper Tu4.6.4.
12. S. Takasaka, and R. Sugizaki, "Polarization Insensitive Fiber Optical Parametric Amplifier Using a SBS Suppressed Diversity Loop," in *Optical Fiber Communication Conference* (Optical Society of America, 2016) paper M3D.4.
13. M. F. C. Stephens, V. Gordienko, and N. J. Doran, "20dB Net-Gain Fiber Optical Parametric Amplification of 18x120Gb/s Polarization-Multiplexed Signals," in *Optical Fiber Communication Conference* (Optical Society of America, 2017), paper Th4A.1.
14. M. McCarthy, N. Mac-Suibhne, S. T. Le, P. Harper, and A. D. Ellis, "High spectral efficiency transmission emulation for non-linear transmission performance estimation for high order modulation formats," in *European Conference on Optical Communication (ECOC 2014)*, paper P.5.7.
15. J. M. Fini, and L. E. Gruner-Nielsen, "Dispersion Fluctuation Invariant Fibers," in *Optical Fiber Communication Conference* (Optical Society of America, 2014) paper Tu2K.2.
16. J. Hansryd, P. A. Andrekson, M. Westlund, J. Li, and P. O. Hedekvist, "Fiber-based optical parametric amplifiers and their applications," *IEEE J. Sel. Top. Quantum Electron.* **8**(3), 506–520 (2002).
17. M. F. C. Stephens, A. Redyuk, S. Sygletos, I. D. Phillips, P. Harper, K. J. Blow, and N. J. Doran, "The Impact of Pump Phase-Modulation and Filtering on WDM Signals in a Fibre Optical Parametric Amplifier," in *Optical Fiber Communication Conference* (Optical Society of America, 2016), paper W2A.43.
18. J. M. Chavez Boggio, A. Guimarães, F. A. Callegari, J. D. Marconi, and H. L. Fragnito, "Q penalties due to pump phase modulation and pump RIN in fiber optic parametric amplifiers with non-uniform dispersion," *Optics Communications* **249**(4), 451–472 (2005).
19. A. Mussot, A. Durécu-Legrand, E. Lantz, C. Simonneau, D. Bayart, H. Maillotte, and T. Sylvestre, "Impact of pump phase modulation on the gain of fiber optical parametric amplifier," *IEEE Photon. Technol. Lett.* **16**(5), 1289–1291 (2004).
20. J. M. Chavez Boggio, J. D. Marconi, and H. L. Fragnito, "Experimental and Numerical Investigation of the SBS-Threshold Increase in an Optical Fiber by Applying Strain Distributions," *J. Lightw. Technol.* **23**(11), 3808–3814 (2005).
21. Z. Lali-Dastjerdi, T. Lund-Hansen, N. Kang, K. Rottwitt, M. Galili, and C. Peucheret, "High-Frequency RIN Transfer in Fibre Optic Parametric Amplifiers," in *Conference on Lasers and Electro-Optics Europe (CLEO-Europe 2011)*, paper CI2.5.
22. M. Jamshidifar, A. Vedadi, and M. E. Marhic, "Reduction of Four-Wave-Mixing Crosstalk in a Short Fiber-Optical Parametric Amplifier," *IEEE Photon. Technol. Lett.* **21**(17), 1244–1246 (2009).
23. R. Elschner, T. Richter, and C. Schubert, "Characterization of FWM-induced Crosstalk for WDM Operation of a Fiber-Optical Parametric Amplifier," in *European Conference on Optical Communication (ECOC 2011)*, paper Mo.1.A.2.
24. M. F. C. Stephens, I. D. Phillips, P. Rosa, P. Harper, and N. J. Doran, "Improved WDM performance of a fibre optical parametric amplifier using Raman-assisted pumping," *Opt. express* **23**(2), 902–911 (2015)
25. A. Redyuk, M. F. C. Stephens, and N. J. Doran, "Suppression of WDM four-wave mixing crosstalk in fibre optic parametric amplifier using Raman-assisted pumping," *Opt. express* **23**(21), 27240–27249 (2015).
26. M. E. Marhic, N. Kagi, T. K. Chiang, and L. G. Kazovsky, "Broadband fiber optical parametric amplifiers," *Opt. Lett.* **21**(8), 573–575 (1996).

1. Introduction

A single-pump Fiber Optical Parametric Amplifier (FOPA) has recently been demonstrated offering exceedingly wide bandwidth (>100 nm) with low signal gain variation (GV) whilst amplifying optical data [1]. This result, together with many others over the preceding 35 years [2–4], shows the undoubted potential of the FOPA as a next-generation optical communications amplifier, but also highlights real-world employability issues due primarily to polarization-dependent signal gain characteristics.

Numerous techniques have been investigated for achieving polarization insensitive (PI) FOPA operation, such as propagating two orthogonally-polarized pumps at symmetrical frequencies about the zero dispersion wavelength (ZDW) of a highly nonlinear fiber (HNLF) [5,6]. This scheme is experimentally complex, but has been shown to work well for optical phase conjugation (OPC) applications. For example, OPC of eight 256 Gb/s polarization-division multiplexed (PDM) signals (0.4 THz total bandwidth) was recently demonstrated, achieving 10 dB on-off parametric gain for the original signals [7]. However, substantial PI net-gain and/or >terahertz gain bandwidth for PDM signal amplification has yet to be experimentally demonstrated using two pumps. This is primarily because it is difficult to apply or maintain any *known* fixed polarization relationship of two pumps within HNLF apart from

a) linearly co-polarized pumps (achieved by maximizing pump-pump mixing) which does not offer PI gain or b) linearly orthogonal pumps (achieved by minimizing pump-pump mixing). However it has been shown that linear orthogonality severely limits achievable PI signal gain [8]. The level of gain can be improved by instead employing orthogonal left/right circular pump polarizations, but this has so far not been demonstrated beyond simulations [8].

A simpler technique for PI operation is to effectively operate two orthogonal single-pump FOPAs in parallel using an interferometric arrangement – e.g. a Mach-Zehnder interferometer using a length of HNLF in each arm (but requiring active path alignment) or a ‘diversity-loop’ Sagnac interferometer arrangement with a single length of HNLF. The diversity loop has been successfully demonstrated using PDM signals for OPC applications [9,10], but is inherently limited for FOPA net-gain amplification due to pump distortions arising from Stimulated Brillouin Scattering (SBS) and Four-Wave Mixing (FWM) of bi-directional pump components [11].

Recently, a novel single-pump FOPA design was demonstrated which significantly reduced the bidirectional pump SBS, allowing stable continuous wave (CW) operation with a low polarization dependent gain (PDG) of ~ 0.5 dB [12]. The design employed dual HNLF lengths within a standard diversity loop, but importantly used WDM filtering to remove the pump in both directions after each first length of HNLF. Importantly, this limited the pump to just a single propagation direction within each HNLF, avoiding the SBS/FWM interaction. We term this architecture the Half-Pass Loop FOPA or HPL-FOPA, owing to each pump propagating through only half the total HNLF. We recently reported the first black-box amplification of PDM signals using an HPL-FOPA [13].

In this paper, we considerably extend this work by employing a commercial 127 Gb/s line-rate (100 Gb/s data-rate) PDM-QPSK transponder in conjunction with twenty-two 100 GHz-spaced emulated signals to thoroughly assess the OSNR and bit error rate (BER) performance following a record aggregate PI-FOPA equivalent data amplification of 2.3 Tb/s. We report an average OSNR penalty at 10^{-3} BER of only 0.5 ± 0.3 dB across all signals for an average 15 dB net-gain. Worst case penalty is 0.8 ± 0.3 dB. We additionally characterize the evolution of FWM crosstalk growth in this HPL-FOPA as the gain and signal output power are independently varied.

2. Experimental Setup

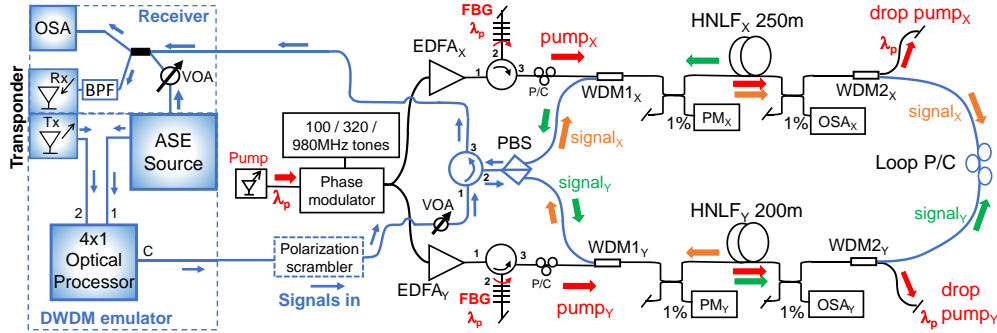


Fig. 1. Schematic of HPL-FOPA experimental setup. ASE = amplified spontaneous emission; VOA = variable optical attenuator; EDFA = erbium doped fiber amplifier; OSA = optical spectrum analyzer; PM = power meter; WDM = wavelength division multiplexing filter; FBG = fiber Bragg grating; BPF = bandpass filter; HNLF = highly nonlinear fiber; PBS = polarization beam splitter; P/C = polarization controller.

The experimental setup is shown schematically in Fig. 1. A commercial Oclaro transponder was employed as both a single-frequency transmitter (Tx) and coherent receiver (Rx). The Tx section produced PDM-QPSK data ($2^{31}-1$ pseudo-random binary sequence) with a line-rate of

127.156 Gb/s. The line-rate included $\sim 20\%$ overhead for soft-decision forward error correction (SD-FEC) and was tuneable across the C-band with 50 GHz granularity. The Rx incorporated an integrated tuneable local oscillator and associated optics, electronics and real-time digital signal processing (DSP) to enable the pre-FEC BER (real, not estimated) to be recorded via a serial interface port. This was shown to provide repeatable back-to-back (B2B) BER performance versus wavelength, OSNR and received power (0 dBm to -20 dBm) for BERs $> 10^{-7}$. To emulate a full set of DWDM signals, the transponder output signal at frequency f_{isp} was routed through an optical processor (Finisar Waveshaper – port 2) and combined with broadband ASE (port 1) at the common (C) output port. The Waveshaper was programmed to shape the ASE and accurately replicate the transponder spectrum to 1 GHz resolution, providing 22x100 GHz-spaced and levelled neighbouring noise channels, whilst blocking the ASE at f_{isp} in a 100 GHz notch. Shaped-ASE signals have previously been shown to conservatively emulate DWDM QPSK performance with slight overestimation of neighboring channel impact [14]. A suite of Waveshaper profiles were thus produced allowing the transponder to be tuned across the C-band on a 100 GHz-spaced DWDM grid from 1532.7 nm (195.6 THz) to 1550.1 nm (193.4 THz) – this represents an equivalent total data throughput of 2.3 Tb/s. An additional profile was also produced for each f_{isp} with the ASE blocked in two 100 GHz windows at $f_{isp} \pm 200$ GHz in order to interpolate the noise floor at f_{isp} for received OSNR measurements, whilst retaining the nearest neighboring signals. In this way the transponder did not have to be disconnected or turned off to measure OSNR. A polarization scrambler was optionally used at the input to explore the polarization sensitivity of the FOPA. The total optical signal launch power level was adjusted using a variable optical attenuator (VOA).

The HPL-FOPA signal path consisted firstly of an input circulator (port 1 to port 2) and polarization beam splitter (PBS) to separate the signals into orthogonal polarization components before propagation in opposite paths X and Y about the loop. The combined insertion loss of these first two components was 0.7 dB. Signals_{X/Y} were then coupled respectively with a pump_{X/Y} using a 200 GHz-wide high-power tolerant thin-film WDM filter (WDM1_{X/Y}) centred at 1563.8 nm and with insertion loss of 0.4 dB. Each pump_{X/Y} was derived from a 100 kHz linewidth tuneable laser of wavelength λ_p which had been phase modulated with RF tones at 100, 320 and 980 MHz to mitigate HNLf stimulated Brillouin scattering (SBS). The relative intensity noise (RIN) of the pump laser was < -145 dB/Hz in a frequency range of 10 MHz to 40 GHz. The pump was split in a 50:50 ratio and both halves amplified in high power EDFAs to allow individual pump power control in each path. Each amplified pump_{X/Y} was filtered to remove excess ASE using a circulator and reflective apodized fiber Bragg grating (FBG) of ~ 1 nm bandwidth centred at λ_p . Each pump_{X/Y} was polarization controlled before combination with signals_{X/Y} using WDM1_{X/Y} respectively. The combined pump and signals in each path_{X/Y} were then passed sequentially through: a 2x2 1% tap for input power and SBS back-reflection monitoring; a length of HNLf_{X/Y} as parametric gain medium; a 1% tap for spectral monitoring via an optical spectrum analyser (OSA); and a second WDM2_{X/Y} to remove the pump_{X/Y}. Both paths_{X/Y} were then spliced together via a common loop polarization controller allowing the amplified signals_{X/Y} each a return path back to the PBS through the second unpumped (in that direction) HNLf. Both paths were re-combined at the PBS allowing the amplified signals to exit via the original circulator (port 2 to port 3).

The HNLf used in the HPL-FOPA was commercially-sourced and possessed low dispersion variation with length [15]. The key parameters were: ZDW ≈ 1564 nm; dispersion slope ≈ 0.084 ps/(nm².km); and nonlinearity $\gamma \approx 8.2$ (W.km)⁻¹. Different lengths of HNLf were used for the two path_{X/Y} gain sections (HNLf_X = 250 m / 1.4 dB and HNLf_Y = 200 m / 0.9 dB) to attempt to compensate for different splice and loop loss distributions in each path direction. The entire signal path was fusion spliced with total passive input to output unpumped loss of 5.5 dB at 1550 nm. The generated idlers remained present in the output spectrum but are not considered for this work.

2.1. Operating principle

The HPL-FOPA was operated as a black-box amplifier by monitoring the signal gain in each path_{X/Y} using the respective OSA_{X/Y} at the output of each HNLF_{X/Y}. The power of each pump_{X/Y} was adjusted in a predetermined proportion (see Section 3.1) so the signal gain in each path compensated for the loss distribution before and after each HNLF when the pump and signals were co-polarized (i.e. at the maximum gain condition for that path). For the amplifier under test, this power ratio was found to be 1 dB. The absolute pump power levels used in this ratio then determined the magnitude of the gain. The HPL-FOPA output power could then be maximized using the loop polarization controller to allow maximum transmittance through the PBS to the circulator and output. At the transponder Rx, the signals were optionally noise-loaded using broadband ASE to degrade the received OSNR before bandpass filtering and detection for BER measurement. Due to non polarization-maintaining fibers being used in this HPL-FOPA, the pump and loop polarization controllers required occasional small adjustments to maintain the gain ratio in the presence of slow thermal and vibrational drifts. Signal polarization was never controlled unless deliberately being scrambled.

3. Experimental Results

To allow for consistent testing of the HPL-FOPA under different conditions, three different pump power combinations were employed to achieve three distinct signal gain regimes. These are termed ‘Low’, ‘Medium’ and ‘High’, and are listed in Table 1. The combinations are used exclusively throughout this paper and equate to average net-gains of 10 dB, 15 dB and 20 dB across the amplified bandwidth *for this set of signals* (i.e. 193.4 – 195.6 THz). Average on-off gain is defined as the linear power difference of each signal between pump-on and pump-off conditions, averaged over all 23 signals and expressed in dB. Average net-gain is the real-world ‘blackbox’ amplifier gain and is calculated as the input-fiber to output-fiber gain per signal, similarly averaged over all the signals. Net-gain is also simply on-off gain minus the total passive loss (in dB).

Table 1. Pump power regimes used for HPL-FOPA gain characterization

Pump power regime	Pump _X (dBm)	Pump _Y (dBm)	Average on-off gain (dB)	Average net-gain (dB)
‘Low’	33.9	32.9	15.5	10
‘Medium’	35	34	20.5	15
‘High’	36.3	35.3	25.5	20

Figure 2(a) shows example HPL-FOPA output power spectra as the pumps_{SX/Y} are adjusted between the three power regimes whilst keeping a fixed pump wavelength (λ_p) of 1564.4 nm. The input power per signal was also fixed at -20 dBm and an OSA resolution bandwidth (RBW) of 0.02 nm used. With the pumps switched off, the output power was simply the input spectrum attenuated by the 5.5 dB total passive loss (producing -25.5 dBm per signal) and is shown by the dark grey trace. This illustrates the semi-transparent nature of the HPL-FOPA, which could potentially allow concatenation of FOPAs with different gain spectra. For this signal input power, out of band FWM crosstalk is low even in the ‘High’ pump power case where the signals have been amplified to 0 dBm average power which is a typical launch power for optical transmission systems. The crosstalk generation will be examined more systematically in Section 3.2.

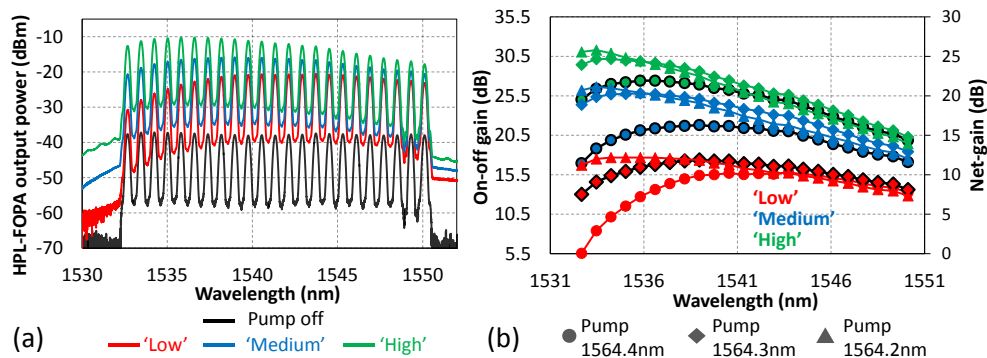


Fig. 2. (a) HPL-FOPA calibrated output spectra for four pump power regimes: off, 'Low', 'Medium' and 'High' as defined in Table 1. $\lambda_p = 1564.4$ nm; $f_{sp} = 1549.3$ nm (193.5 THz) and -20 dBm per signal input power. (b) Signal gain spectra (both on-off and net-gain shown) for 'Low', 'Medium' and 'High' pump regimes as defined in Table 1. The spectra highlighted in black were chosen for subsequent experiments as the flattest for each regime.

Figure 2(b) shows both the net and on-off signal gains as the pump wavelength (λ_p) is varied for each pump power regime. As the pump power is increased, the gain bandwidth is seen to significantly broaden as per standard FOPA behavior [15], and the gain peak moves away from the pump to lower wavelengths. This implies that many more signals could be amplified using this FOPA beyond the C-band. The signal gain at a particular wavelength is seen to rise nonlinearly in dB compared to other wavelengths as the phase matching conditions are altered [16]. For a fixed pump power, a lower wavelength λ_p is also seen to enhance gain at the low wavelength end of the spectrum, extending the FOPA bandwidth towards the S-band. For the shortest pump wavelength ($\lambda_p = 1564.2$ nm) this also caused decreased gain at the high wavelength end. Ongoing characterization was hence undertaken using $\lambda_p = 1564.4$ nm for 'high' and 'medium' pump powers, and $\lambda_p = 1564.3$ nm for 'low' as these produced the flattest spectra for this signal distribution and pump powers.

3.1. BER characterization of HPL-FOPA

The authors consider that the ultimate metric for assessing the performance of current FOPAs is the impact on BER suffered by an optical signal amplified by that FOPA when compared with the non-amplified version. This is because there are numerous sources of potential penalty which cannot be captured via conventional measures such as optical noise figure. These sources would include pump-to-signal RIN or phase modulation (PM) transfer for example [17-19]. In the specific case of the HPL-FOPA, there is an additional potential source of penalty arising from non-optimized gain in the two paths_{X,Y} about the loop. As a result, we present both single channel and DWDM characterization results using the transponder BER to tabulate the HPL-FOPA performance, including its polarization sensitivity. Additionally, this reflects operation within a real-world transmission system.

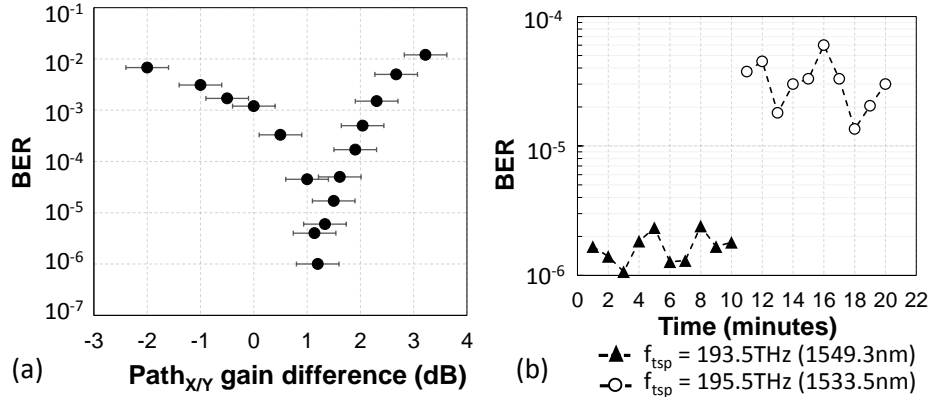


Fig. 3. (a) Graph showing change in transponder BER (1549.3 nm/193.5 THz) as the path_{XY} gain difference ($gain_X - gain_Y$) of the HPL-FOPA is changed. (b) Graph of transponder BER (1549.3 nm/193.5 THz) against time as signal polarization scrambled.

Firstly, to characterize the impact of non-optimum pump power/gain about the two HPL-FOPA paths, the transponder was set to $f_{tsp} = 193.5$ THz (1549.3 nm) and the BER measured as the pump power in each path was varied. This was achieved by first setting the on-off gain in one path of the loop to 15.5 dB (10 dB net gain) by pump power adjustment in that path. The gain in the other path was then varied by ± 3 dB, before switching the fixed path and repeating the measurement. The change in BER with path_{XY} gain difference is shown in Fig. 3(a) for the combined results. The estimated x-axis error bars are relatively large at ± 0.4 dB due to two subtractions being required to calculate the gain-difference. The BER is seen to be minimized at a path difference of 1.1 ± 0.4 dB, which corresponds well with the loop pre/post HNLF path loss difference of ~ 1 dB discussed earlier. If the wavelength-dependent FOPA insertion loss variation across the gain bandwidth is small, and the gain characteristics of the two HNLF lengths matched, this optimal gain-difference can be used for each pump power regime and signal wavelength within this range. However, the steep roll-off from the optimum point is also clear, and the sensitivity of the required gain-difference could prove a limiting factor for significantly extending the DWDM bandwidth. A real-world HPL-FOPA based on this architecture would also require accurate photodiode calibration and responsive pump control. This is considered to be feasible, engineering-wise.

To determine the sensitivity of the HPL-FOPA to signal polarization, the loop was maintained at the optimum path_{XY} gain difference and the transponder signal continuously polarization scrambled. Small adjustments were periodically made to the pump and loop polarization controllers to maintain the ratio in the presence of slow thermal drifts. These adjustments were made without knowledge of the BER at the receiver. The BER was sampled at one minute intervals for ten minutes before the signal frequency was tuned to the opposite end of the band (195.5 THz) and the process repeated. The BER evolution is plotted in Fig. 3(b) showing only minor fluctuations with time at both extremes of the band. It can therefore be considered that the HPL-FOPA offers effective PI amplification. It can be seen that the BER was significantly worse at the short wavelength (high frequency) end of the band, and this will be discussed in detail below. It should also be noted that the variation in BER was $\sim 2x$ larger at the shorter wavelength which may be due to the larger gain changes experienced by a signal located at this part of the spectrum when pump power is varied by a fixed amount [see Fig. 2(b)]. Polarization dependent gain (PDG) obtained using a scrambled polarized CW laser as input source was found to be 0.4 dB at 1542.1 nm (194.4 THz), but was not measured across the whole gain spectrum due to time constraints. The long-term stability of the HPL-FOPA would be much improved using polarization-maintaining fibers [12].

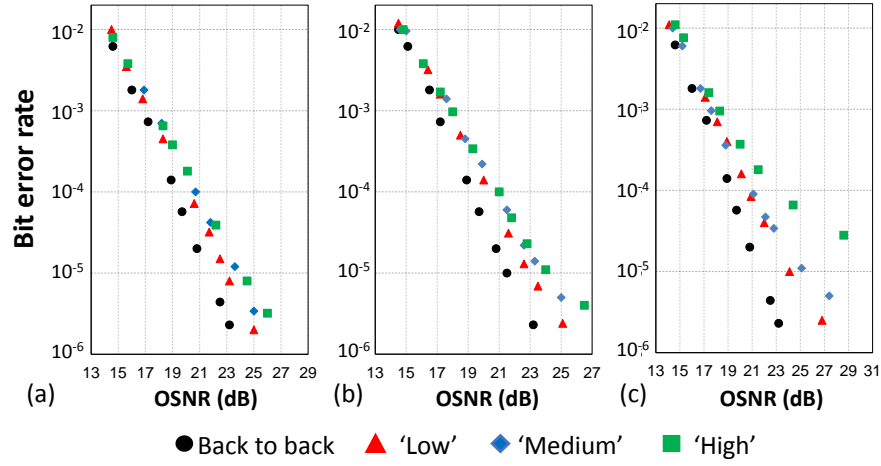


Fig. 4. BER against received OSNR under ‘Low’, ‘Medium’ and ‘High’ HPL-FOPA pump power conditions for (a) $f_{isp} = 193.5$ THz (1549.3 nm), (b) $f_{isp} = 194.5$ THz (1541.4 nm), (c) $f_{isp} = 195.5$ THz (1533.5 nm). A comparison with the back-to-back transponder performance at each f_{isp} is included for each condition.

For amplification of the full twenty three DWDM signals simultaneously, the BER is plotted against received OSNR in Fig. 4 for three representative signals across the FOPA bandwidth ($f_{isp} = 193.5$ THz, 194.5 THz and 195.5 THz) under the three pump power regimes. Polarization scrambling was not used for these measurements. The results show acceptable performance across the band for both the ‘Low’ and ‘Medium’ pump regimes in comparison with the back to back transponder. For a fixed received BER of 10^{-3} , the OSNR penalty is <1 dB under these conditions. Considering instead a fixed OSNR, the BER is seen to generally degrade as both the pump power and frequency separation of the signal from the pump are increased. There is a hint of an emerging error floor for the ‘Medium’ pump power at $f_{isp} = 195.5$ THz, which then develops significantly under ‘High’ power pumping. The increase of the penalty with both pump power and frequency separation of pump and signal is consistent with previous results in single-polarization FOPAs whereby the pump phase modulation used to counteract SBS causes rapid gain and phase changes to the signals, impacting performance [17-19]. It is hoped that future research into strained HNLf [20], will reduce or eradicate this penalty source as currently it is unavoidable in a single pump FOPA employing pump phase modulation. It should also be noted from Fig. 2 that as the pump power is increased, the gain of the low wavelength signals increases much faster than the high wavelengths owing to their position relative to the gain peak. This would strengthen any pump to signal noise mechanisms such as the transfer of pump RIN [21]. Other sources of penalty are remnant ASE from the high power EDFA used to amplify the pump, and signal-signal FWM. Together these issues are certainly not insurmountable and could be improved respectively using a lower-RIN pump laser, tighter pump filtering and shorter HNLf lengths [22]. Finally, the increased degradation at short wavelengths and high gains *is not attributed* to loop gain imbalances (PDG) within this FOPA, although there may be a small component resulting from this. This was confirmed during subsequent experiments whereby attempts were made to remove the penalty by re-balancing the loop, and this was found to be not possible under any combination of $path_{XY}$ gains.

Figure 5 shows the wavelength response of the HPL-FOPA BER performance for all twenty-three signals in the ‘Medium’ pump regime (15 dB net-gain) and with average input power per signal of -15 dBm. The transponder was swept through all twenty three frequencies while the Waveshaper profile was also re-programmed for each to keep the emulated DWDM signal count constant. The OSNR required to obtain 10^{-3} BER is plotted against wavelength for each signal and for the back-to-back (B2B) transponder. The transponder shows a small back

to back increase in required OSNR towards shorter signal wavelengths although this is within the measurement error. Following amplification in the HPL-FOPA, additional OSNR is required at each signal wavelength to accomplish the same BER as B2B. For signals >1540 nm (the FOPA gain peak wavelength), the additional OSNR required is fairly constant at $\sim 0.5 \pm 0.3$ dB, but for <1540 nm this rises to a maximum of 0.8 ± 0.3 dB for $f_{isp} = 195.6$ THz (1532.7 nm). The average OSNR penalty over all twenty three signals is 0.5 ± 0.3 dB to achieve 10^{-3} BER. The total equivalent data throughput for this amplification was 23×100 Gb/s or 2.3 Tb/s which we believe is the highest yet reported for a FOPA of any variant.

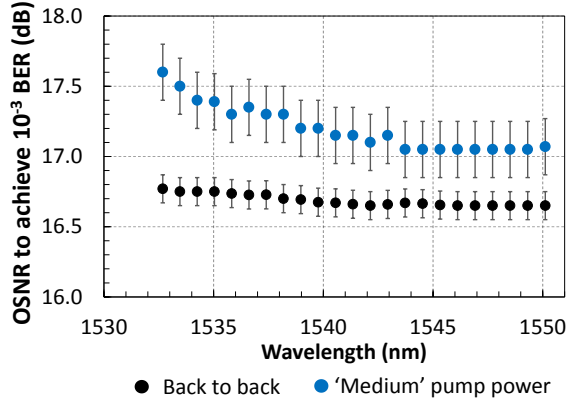


Fig. 5. Graph showing the received OSNR required to achieve a BER of 10^{-3} against wavelength in both back to back and 'Medium' pump power (~ 15 dB net-gain) configurations. Measurement error is estimated to be ± 0.1 dB and ± 0.2 dB respectively.

3.2. FWM crosstalk growth

For potential use as a signal amplifier within a DWDM system, understanding the generation of signal-signal and signal-pump mixing products within the HPL-FOPA is important as this crosstalk can reduce the effective OSNR at the receiver, and degrade the BER [23]. As such, the experimental setup of Fig. 1 was altered to incorporate a launch signal EDFA_{sig} before the FOPA (replacing the polarization scrambler). The input power of the twenty three signals into the FOPA could then be adjusted to a maximum of +10 dBm per signal to explore the crosstalk generation in two distinct cases: i) unpumped – with no parametric pump or FOPA gain in either HNLFX_Y and using high signal input powers to the HPL-FOPA via EDFA_{sig}; ii) pumped under the three standard pump regimes giving parametric net-gain of 10/15/20 dB and using lower signal input powers to achieve similar output powers to the unpumped case. This allows a comparison to be made between the crosstalk levels in the two cases.

The spectra of Fig. 6(a) show the crosstalk growth in the unpumped case for four different FOPA signal *output* powers. Three spectra are taken for each power with one channel removed each time (193.5 THz, 194.5 THz or 195.5 THz) to illustrate the crosstalk generated at each frequency. Figure 6(a) shows that the signal at 1541.4 nm (194.5 THz) suffers maximum crosstalk growth due to possessing the most neighbors. Figure 6(b) plots the signal to crosstalk (S/XT) ratio (measured in 0.02 nm RBW) for the central channel against the output power per signal. It can be seen that the S/XT ratio starts to decrease rapidly for output powers greater than -7 dBm per signal. It should be noted that there are *no idlers present* in this unpumped case and that the signal power in both lengths of HNLFX_Y is higher than the signal output power due to passive loss.

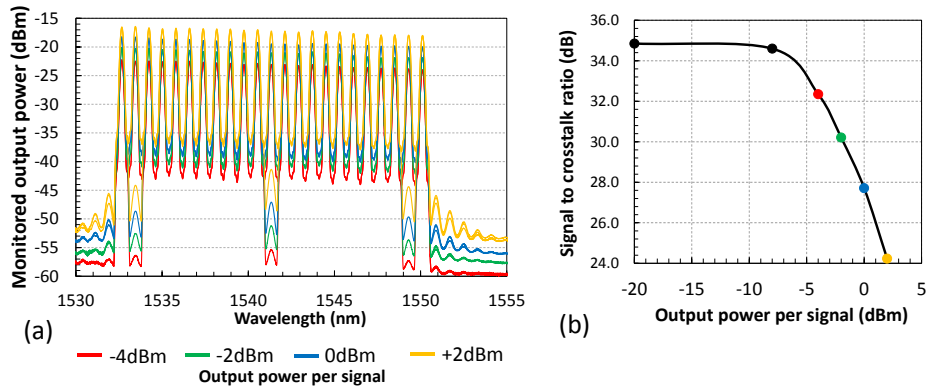


Fig. 6. (a) Tap-monitored output power spectra from the HPL-FOPA with pump turned off and output power per signal varied from +1 dBm to +7 dBm (OSA RBW = 0.02 nm). (b) Signal peak to crosstalk ratio vs signal output power for HPL-FOPA with pump turned off at 1541.4 nm (194.5 THz). Colors correspond to Fig. 6(a).

Alternatively in the pumped case, the signal input power to the HPL-FOPA is much lower, even though the output power is the same due to the gain experienced by the signals. The signal power thus undergoes a considerably different evolution versus propagation length [24,25]. As such, it might be expected that crosstalk growth be reduced over the unpumped case for the same output power because the signals are at lower power for a higher proportion of propagation distance, thus producing less nonlinearity. However the situation is complicated by the presence of idlers in the pumped case which effectively doubles the signal count and thus the total signal-signal FWM interaction power. This will be analyzed in Section 3.3.

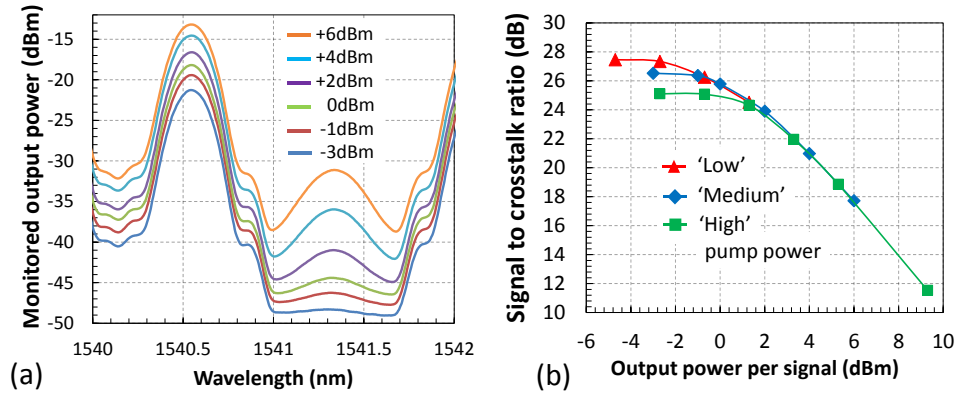


Fig. 7. (a) Tap-monitored output power spectra from the HPL-FOPA under fixed 'Medium' pump power condition (15 dB net-gain) as output power per signal varied from -3 dBm to +6 dBm (OSA RBW = 0.02 nm). (b) Signal peak to crosstalk ratio at 1541.4 nm (194.5 THz) against signal output power for HPL-FOPA under the three pump power conditions 'Low', 'Medium' and 'High' (10 dB, 15 dB and 20 dB net-gains).

Figure 7(a) shows spectra at different signal output powers under the 'Medium' fixed pump power regime and with the central 194.5 THz channel removed. By comparing the '+2 dBm' purple spectra with the same power trace (orange) in Fig. 6(a) it can be seen that the signal and crosstalk peaks are both very similar in power, giving the same S/XT ratio in both the pumped and unpumped case (albeit with ~3 dB extra interaction power in the pumped case due to idlers). Figure 7(a) additionally shows that the crosstalk level becomes masked at lower signal output powers by other noise such as amplified ASE. This effectively limits the S/XT ratio to a

maximum of ~27 dB, compared to ~35 dB in the unpumped case, which essentially offers an indication of HPL-FOPA noise figure in the absence of crosstalk.

In Fig. 7(b), the S/XT ratio of the three different pump power regimes are plotted against signal output power with some crossover of signal power arranged between the pump regimes to allow comparison. It can be seen that all the points lie on the same curve, indicating that crosstalk growth is gain independent at a fixed signal output power for the central signal under these conditions. However, the gain level is seen to impact the maximum S/XT ratio achievable. This is most likely due to increased remnant ASE from the pump EDFA as the EDFA gain was increased.

3.3. HPL-FOPA effective length

A consideration of HPL-FOPA effective length (L_{eff}) was undertaken to help illustrate the relative significance of the two respective HNLf sections at producing crosstalk for fixed signal output power. It also allowed estimation of relative nonlinearity under different gains at fixed signal output power.

We define L_{eff} according to Eq. (1), where $P(z)$ is the signal power at a particular propagation distance z through the HPL-FOPA, and L is the total length of a single path through the HPL-FOPA. We choose to model a linear power dependence as a conservative estimate of the nonlinear impact and we also normalize the integrated power profile to the signal *output* power $P(L)$ as per the experiments, measured at the output of the HPL-FOPA. This has the effect of producing effective lengths longer than the physical length. Only uni-directional propagation is considered in this model for simplicity.

$$L_{eff} = \frac{\int_0^L P(z) dz}{P(L)} \quad (1)$$

Using knowledge of the component insertion losses, splice losses and HNLf attenuation coefficient detailed in Section 2, the loss experienced by the signals in the HPL-FOPA were estimated and a power profile ‘map’ generated and numerically integrated according to Eq. (1). Two configurations were modelled in this way:

1. As per the experiments described in this paper, the first HNLf in the path parametrically pumped with the second HNLf kept passive.
2. The first HNLf kept passive, and the second HNLf parametrically pumped.

In the presence of parametric gain, Eq. (1) was modified so that $P(z) = P_s(z) + P_i(z)$, where $P_s(z)$ and $P_i(z)$ were the length-dependent signal and idler powers respectively. Normalization for L_{eff} was maintained relative to signal output power only. The signal and idler power at position z was calculated in 1 m steps according to Eq. (2), where z_0 refers to the beginning of the relevant pumped HNLf section and r is a gain parameter (γP) numerically adjusted to achieve the required on-off gain within the particular HNLf being pumped. Equation (2) is derived according to standard FOPA equations for signal gain and signal-to-idler conversion efficiency [26].

$$P_s(z) = P_s(z_0) \times |\cosh(rz)|^2 \quad \text{and} \quad P_i(z) = P_s(z_0) \times |\sinh(rz)|^2 \quad (2)$$

The power profiles for signal and idler are shown in Fig. 8(a) for an example case of 20 dB net-gain and signal output power of 20 dBm.

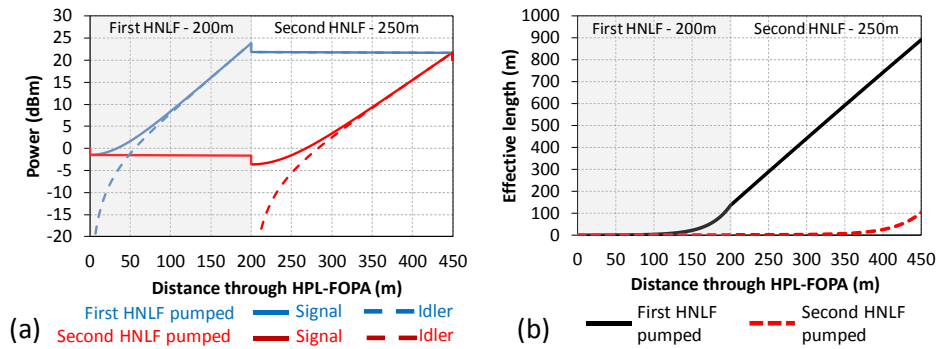


Fig. 8. (a) Power profiles against propagation distance for two configurations of HPL-FOPA, both with 20 dB net-gain and output power of 20 dBm. Blue configuration has the first 200 m HNLf pumped. Red configuration has second HNLf pumped (b) Effective length against distance through the HPL-FOPA for the same two configurations.

It can be seen that the idler reaches power parity with the signal after ~100 m of HNLf in both configurations. With the first HNLf in the path pumped, the combined signal/idler power receives gain early in the propagation and thus sees a much higher integrated power over length than having the second HNLf pumped. This produces extreme differences in L_{eff} at the output of the HPL-FOPA in the two configurations as shown in Fig. 8(b). There is almost an order of magnitude reduction in L_{eff} (885 m to 104 m) observed by moving the gain section to the second HNLf in the path. This would enable a significant reduction in FWM crosstalk within the HPL-FOPA and will be investigated experimentally in future work. Undoubtedly this would also cause a detrimental impact to noise figure by shifting a higher proportion of the loss to the region before the signals see amplification. A trade-off is therefore likely between systematic noise figure penalty and signal-count dependent crosstalk.

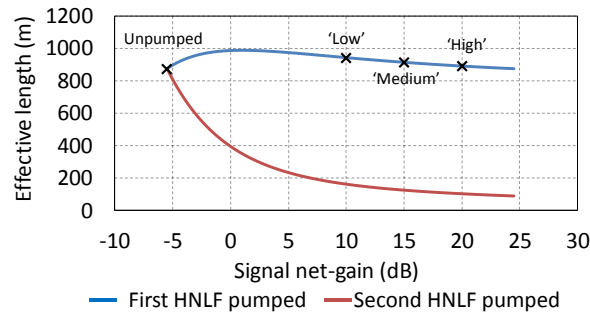


Fig. 9. Graph showing Effective Length (L_{eff}) against signal net-gain for the two HPL-FOPA configurations. The black crosses indicate the gains that were experimentally investigated in Section 3.2.

Finally, L_{eff} at the output of the HPL-FOPA was calculated for the two configurations over a continuous range of signal net-gains from -5.5 dB (unpumped case) to >20 dB pumped. It can be seen that the experimental observation of very similar crosstalk in both unpumped and first HNLf-pumped cases is reproduced in the L_{eff} calculation. L_{eff} values for the unpumped, 10 dB, 15 dB and 20 dB cases are 875 m, 943 m, 914 m and 891 m respectively which is an excellent agreement. Again, it can also be seen that by shifting the parametric gain to the second HNLf in each path, nonlinear crosstalk will be significantly reduced over all gains, and reducing with gain.

Conclusions

A black-box PI-FOPA employing a Half-Pass Loop architecture has been characterized for the first time using a commercial polarization-division multiplexed PDM-QPSK 127 Gb/s transponder. A record total of 23x100 Gb/s equivalent DWDM signals were amplified occupying a 2.3 THz bandwidth within the C-band for three different pump power regimes. The pump regimes produced net-gains of 10 dB, 15 dB and 20 dB when averaged over all signals, with considerable excess bandwidth observed beyond the C-band. We hope to exploit this potential in future work to produce an HPL-FOPA with >50 nm bandwidth. Under the 15 dB gain condition, the worst-case OSNR penalty measured over all signals was only 0.8 ± 0.3 dB (at 10^{-3} BER), highlighting the achievement of polarization independent gain over the band. At higher gain, the penalty was seen to increase, particularly for signal wavelengths at large separation from the pump. This behavior is attributed to the pump phase modulation used to counteract SBS effects. It is expected that the level of phase modulation can be reduced in future work by applying strain gradients to the HNLFs. The growth of four-wave mixing signal-signal crosstalk was additionally characterized in this paper and found to be gain independent for a fixed signal output power. An analysis of the HPL-FOPA effective length predicts this behavior and suggests a method of significantly decreasing unwanted FWM crosstalk using an alternative configuration of pumping the second HNLF in each path instead of the first.

Funding

UK Engineering and Physical Sciences Research Council (EPSRC) (EP/M005283/1); II-VI for CASE studentship of V. Gordienko

Acknowledgments

The authors wish to thank Professor Andrew Ellis of Aston University for useful discussions. Oclaro are thanked for the loan of the transponder used in the experiments. The data reported in this paper is available at <http://doi.org/10.17036/researchdata.aston.ac.uk.00000204> as part of the UK EPSRC open access policy.